inorganics

IMPACT FACTOR 3.1

CITESCORE 2.8

Article

NMR-Based Structural Insights on Folic Acid and Its Interactions with Copper(II) Ions

Arian Kola and Daniela Valensin

Special Issue

Women's Special Issue Series: *Inorganics*

Edited by

Prof. Dr. Tatjana N. Parac-Vogt, Prof. Dr. Sophie Hermans, Prof. Dr. Sandra Luber and Dr. Christelle Hureau

MDPI

https://doi.org/10.3390/inorganics12090248

inorganics

MDPI

Article

NMR-Based Structural Insights on Folic Acid and Its Interactions with Copper(II) Ions

Arian Kola and Daniela Valensin *

Department of Biotechnology, Chemistry and Pharmacy, University of Siena, Via Aldo Moro 2, 53100 Siena, Italy; arian.kola@unisi.it

* Correspondence: daniela.valensin@unisi.it; Tel.: +39-05-7723-2428

Abstract: Folic acid (FA) is an essential vitamin involved in crucial metabolic processes, while copper(II) ions play significant roles in various biological functions. This study aims to investigate the interaction between FA and Cu^{2+} using ^{1}H and ^{13}C NMR spectroscopy under different pH levels and concentrations. The research employed detailed NMR analysis to explore how Cu^{2+} binds to FA, focusing on changes in chemical shifts, diffusion coefficients, and copper-induced paramagnetic effects. The key findings reveal that Cu^{2+} predominantly coordinates with the pteridine ring (PTE) of FA, with minimal involvement from the glutamic acid (Glu) moiety. The interaction is strongly concentration-dependent: at lower FA concentrations, Cu^{2+} binds effectively to the PTE ring, while at higher concentrations, intermolecular interactions among FA molecules hinder copper binding. The study also observed pronounced paramagnetic effects on the PTE and p-aminobenzoic acid protons, with negligible effects on Glu signals. These results provide new insights into the structural characteristics of FA-Cu^{2+} complexes, contributing to a better understanding of their biochemical interactions and implications for folate metabolism.

Keywords: folic acid; copper(II) ions; NMR spectroscopy; pteridine ring; metal coordination; diffusion coefficients; paramagnetic effects; vitamin B9; structural characterization

Citation: Kola, A.; Valensin, D. NMR-Based Structural Insights on Folic Acid and Its Interactions with Copper(II) Ions. *Inorganics* **2024**, *12*, 248. https://doi.org/10.3390/inorganics12090248

Academic Editors: Tatjana N. Parac-Vogt, Sophie Hermans and Sandra Luber

Received: 25 July 2024
Revised: 3 September 2024
Accepted: 10 September 2024
Published: 12 September 2024

1. Introduction

Folic acid, a pivotal nutrient essential for cellular function, owes much of its early understanding to Lucy Wills. Her pioneering work in the 1930s demonstrated its efficacy in treating macrocytic anemia using yeast extracts. Named after its discovery in spinach by Mitchell in 1941, folic acid gained prominence for its vital role in human health. Its synthesis in 1943 by Bob Stokstad at Lederle Laboratories marked a critical advancement, enabling further research into its biochemical properties and therapeutic applications [1].

Folic acid (FA), also known as vitamin B9, is a crucial water-soluble molecule involved in numerous metabolic processes [2]. Its chemical structure is composed of three distinct moieties: a pteridine ring (PTE), para-aminobenzoic acid (PABA), and L-glutamic acid (Glu). The pteridine ring is a heterocyclic aromatic moiety, which connects to PABA via a methylene bridge, and this assembly is further attached to a single glutamate residue (Scheme 1). The core structure of folic acid, referred to as pteroylglutamic acid or pteroylglutamate (deprotonated form) [3], can undergo various modifications according to pteridine ring reduction, one-carbon substitutions, and different counts of glutamate residues. Among them, the semi or total reduction of the pteridine ring results in two different forms of folate, dihydrofolate (DHF) and tetrahydrofolate (THF). THF is the biologically active form of folate, acting as a carrier of one-carbon units in a variety of critical reactions such as nucleotide synthesis, DNA repair and homocysteine methylation [4–7].

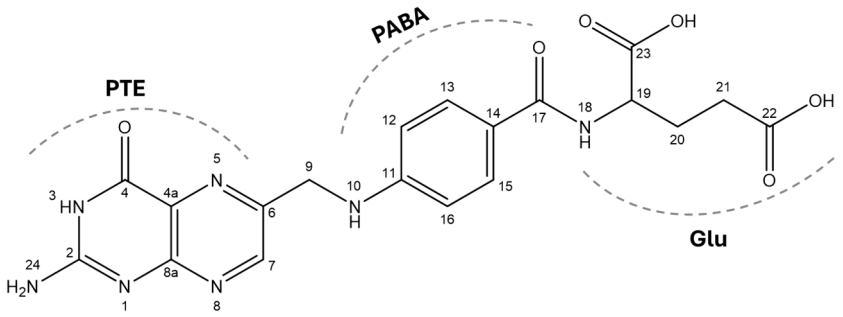

Scheme 1. Molecular structure and atom numbering of folic acid.

Deficits in folic acid are associated with high levels of homocysteine which in turn are correlated with brain dysfunctions observed in Alzheimer's disease (AD) [8–10], vascular dementia [11], stroke [12], cancer [13], and neural tube defects [14].

Folate in foods, like fresh green leafy vegetables, beans, yeast, fruits, and liver, is mainly present as polyglutamates, which need to be hydrolyzed to monoglutamates before absorption. In contrast, folate supplements like (FA) and 5-methyltetrahydrofolate (5-Me-THF) are absorbed directly without needing this modification. Once absorbed, folate monoglutamates from both dietary sources and supplements enter cells through membrane receptors. Inside the cell, they are first converted to dihydrofolate (DHF) and then to the active form, tetrahydrofolate (THF), via reductase enzymes. THF enters the folate cycle where homocysteine is methylated to methionine [15,16].

Folic acid is often taken as a dietary supplement, especially by pregnant women or those planning a pregnancy, to ensure an adequate intake of this vitamin. Folic acid supplements are also used to treat or prevent folate deficiencies. The significance of folic acid in public health is evident in the mandatory fortification of foods in numerous countries, aimed at decreasing the prevalence of nutritional deficiencies among the population. Ongoing scientific research on folic acid emphasizes its importance not only as a crucial nutrient but also as a potential preventive measure against various diseases, reinforcing its essential role in human nutrition and preventive medicine [17–20].

However, FA is not the only essential micronutrient that our body needs to maintain optimal health. In fact, within our bodies, myriad biological processes occur, including electron transfer, oxygen transport, the maintenance of osmotic pressure, and the regulation of DNA transcription, with metals providing a fundamental contribution to their regulation [21].

Essential metals such as iron, copper, zinc, cobalt, selenium, and manganese are crucial for human life, and are typically required in trace amounts. Among these, transition metals like Cu, Zn, and Fe are particularly vital for enzyme activity, neurotransmitter function, and brain aging. The critical role of metals in the human body is underscored by the fact that imbalances, known as metal dyshomeostasis, are linked to various diseases, including neurodegenerative disorders [22–30]. Notably, copper concentrations in cerebrospinal fluid (~70–80 μM) are significantly higher than those in serum (12–24 μM) [31], pointing out a crucial role for copper signaling in the brain. While most copper in the body is tightly bound to proteins, a portion exists in a more loosely bound form, referred to as the free copper or labile copper pool [31–33]. Importantly, labile copper levels are elevated in the brain regions most affected by Alzheimer's disease (AD), and strong evidence suggests that an excessive accumulation of free copper contributes to cognitive decline in AD patients [34].

From the bioinorganic chemistry perspective, the presence of free copper, or loosely bound copper, opens up the possibility for non-specific interactions with biologically active molecules (e.g., amino acids, oligopeptides, vitamins). Such interactions could have significant implications, potentially altering the behavior or function of these biomolecules. Understanding these non-specific copper–ligand interactions could provide new insights into the role of copper in both health and disease, especially in conditions such as neurodegenerative disorders or metabolic imbalances where copper levels are known to be altered.

Metal–folate interactions has been extensively investigated in the scientific literature in recent years [24]. FA has shown the ability to bind several essential metal ions like copper [35–37], iron [35–38], calcium [39], magnesium [39], and zinc [36–38]. The majority of the results agree that all the metal ions coordinate FA through the α and β carboxylate groups of the glutamate moiety, acting as a bidentate ligands. At the same time, it is well known that the PTE moieties can participate to the coordination sphere of several metal complexes through the involvement of N and O donor atoms [40–44].

In order to better understand the relevance of FA-Cu^{2+} interaction, in this study we investigated the copper coordination to FA by using ^{1}H and ^{13}C NMR spectroscopy at different pH and concentrations. Our results have provided a detailed structural characterization of the metal coordination sphere, unequivocally elucidating the role played by pteridine and carboxylate groups. The NMR analysis also allowed to obtain new insights on the chemical features of FA in aqueous solution.

2. Results

2.1. NMR Analysis of Folic Acid: Investigating the Effects of pH and Concentration in Solution

The NMR spectrum of FA 0.5 mM in 20 mM phosphate buffer (pH 7.35) is characterized by the presence of signals of aromatic protons (H7, H12, H13, H15, H16) of PTE and PABA, and the amide and aliphatic protons (H19, H20, H21) of Glu as shown from the ^{1}H signal's assignment reported in Table S1. NMR analysis was also performed recording spectra at variable pH (6.0–8.0) and concentration (0.1–10 mM) values. As expected, pH changes led to chemical shift variations in aromatic protons, namely due to the pKa = 7.85 of the NH at position 3 on the PTE ring (Figure S1). On the other hand, concentration variations in the range 0.1–2 mM led to subtle chemical shift changes in PABA protons, with H12,16 being the most affected ones (Table S1). Further concentration increases up to 10 mM caused larger chemical shift changes, including H7 and H9 nuclei as well.

In order to verify the occurrence of inter-molecular stacking interactions between the aromatic rings, DOSY experiments were performed on FA samples at concentrations ranging from 0.1 to 8 mM. Table 1 shows that concentrations ranging from 0.1 to 1 mM yield roughly the same diffusion coefficient. However, increasing the concentration to 8 mM led to a noticeable increase in the diffusion coefficient, with particularly pronounced effects at 4 mM and 8 mM. The observed trends are consistent with the formation of higher molecular weight species due to π-π stacking, which is typically seen in PABA-containing systems and in FA at high concentrations ranging from 25 to 100 mM [45,46]. The presence of intermolecular interactions is also confirmed by comparing the ^{1}H-^{1}H NOESY spectra recorded at 2 mM and 8 mM concentrations (Figure 1). In fact, the Nuclear Overhauser Effect (NOE) can exhibit different signs depending on the molecular motion in solution. As evident from Figure 1, the two spectra display NOE correlations with opposite signs, reflecting different tumbling rates of FA. Specifically, the change in the sign of the NOEs is consistent with a decreased tumbling rate of FA at higher concentrations.

Table 1. Diffusion coefficient values ($D \times 10^{-10}$ m^2/s) of FA calculated at different concentrations, phosphate buffer 20 mM, T 298 K. The diffusion coefficient of TMSP-d4 is also reported for the purpose of comparison.

C_M (mmolL^{-1})	$D \times 10^{-10}$ m^2s^{-1}	
	FA	**TMSP**
0.1 mM	3.09	4.94
0.5 mM	3.06	4.94
1.0 mM	3.05	4.93
2.0 mM	2.97	4.92
4.0 mM	2.81	4.90
8.0 mM	2.64	4.95

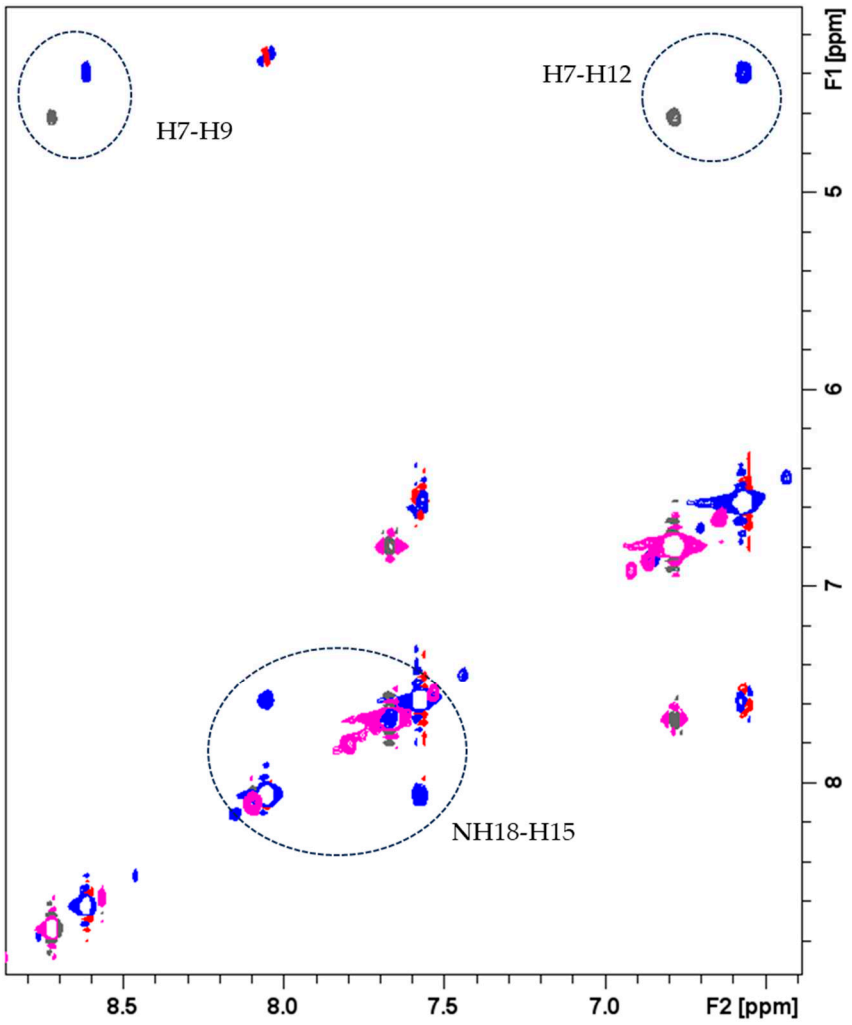

Figure 1. Comparison of ^{1}H-^{1}H NOESY spectra of FA 8.0 mM (blue (+)/red (−) contours) and 2.0 mM (magenta (+)/gray (−) contours). Phosphate buffer 20 mM, pH 7.3, T = 298 K.

2.2. NMR Study of Folic Acid–Cupric Ion Interactions

The interaction between FA and copper was initially explored using ^{1}H NMR spectroscopy, focusing on the copper-induced line-broadening effects, evident for nuclei near the paramagnetic center [47–51]. As shown in Figure 2, copper addition led to the selective broadening of the H7 signal, which almost vanished in the presence of 0.10 Cu^{2+} equivalents (eqs).

No effects are evident on Glu resonances (NH18, H19, H20 and H21), thus excluding copper coordination to the Glu carboxylate groups. Similar NMR titrations spectra of FA were also recorded in the presence of Fe^{3+}, Fe^{2+} and Zn^{2+} which, similarly to Cu^{2+}, are known to form stable metal complex with FA [35–38]. Our data showed the absence of relevant changes in NMR spectra upon any metal addition, strongly indicating the occurrence of no binding for both iron and zinc ions (Figures S2–S4).

The effects of copper were also monitored by examining different FA concentrations to verify whether concentration-dependent binding modes occur. Figure 3 shows the intensity variations (I/I_0) of FA signals upon the addition of 0.02 equivalents of Cu^{2+}. In all cases, the largest paramagnetic effects are observed on the PTE (H7) and PABA (H12, H16, H13, and H15) signals, while the Glu (H20 and H21) signals are barely influenced by the presence of cupric ions. These findings indicate that PTE moieties is the preferential copper-anchoring site for all the tested concentrations. Moreover, by examining the copper-induced line broadening at different concentrations, it is possible to observe a common trend: the higher

the FA concentration, the more pronounced the signal variations, especially for PTE and PABA protons (Figure 3).

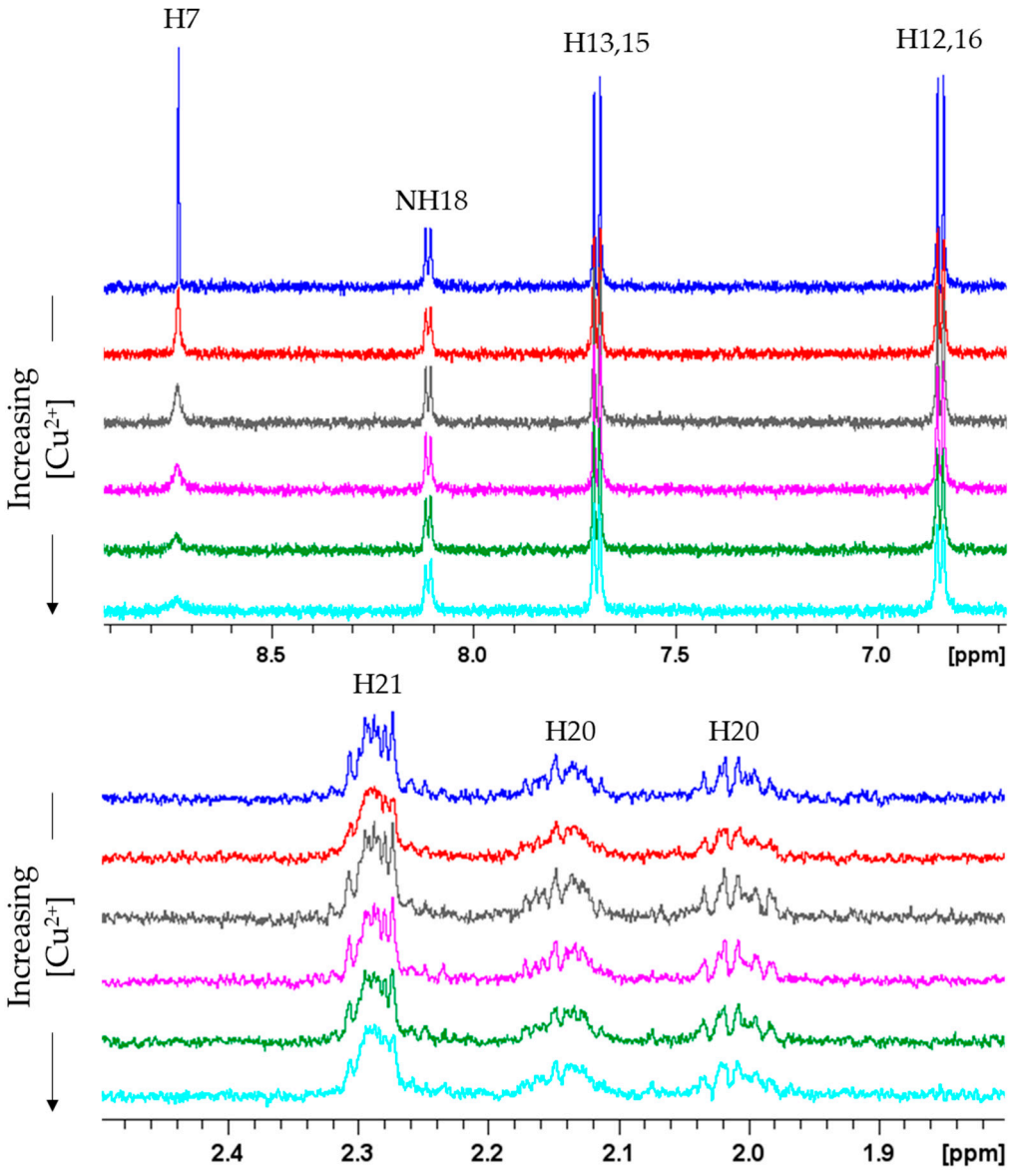

Figure 2. ^{1}H NMR spectra of FA 0.1 mM in phosphate buffer 20 mM (pH 7.35) and T = 298 K in absence and in presence of Cu^{2+} ions. Cu^{2+} = 0 eqs (blue); Cu^{2+} = 0.02 eqs (red); Cu^{2+} = 0.04 eqs (gray); Cu^{2+} = 0.06 eqs (magenta); Cu^{2+} = 0.08 eqs (green); Cu^{2+} = 0.10 eqs (light blue).

A similar trend is observed when measuring the spin-lattice relaxation rates of H7 and H12,16 both in the absence and presence of cupric ions, leading to the determination of the paramagnetic relaxation enhancements (R_{1p}). The obtained values were readily measured at different FA concentrations and are shown in Figure 4. As previously observed with signal intensities, R_{1p} values increase with higher copper concentrations, indicating that concentration-dependent processes are involved in the formation of copper complexes. Specifically, the varying copper concentrations likely lead to differences in the dissociation rates of the copper–folate complex, thereby affecting the overall kinetics of the copper–folic acid reaction (vide infra). In particular, the observed tendency of folic acid to aggregate, as shown by DOSY experiments, likely contributes to the differences in reaction kinetics.

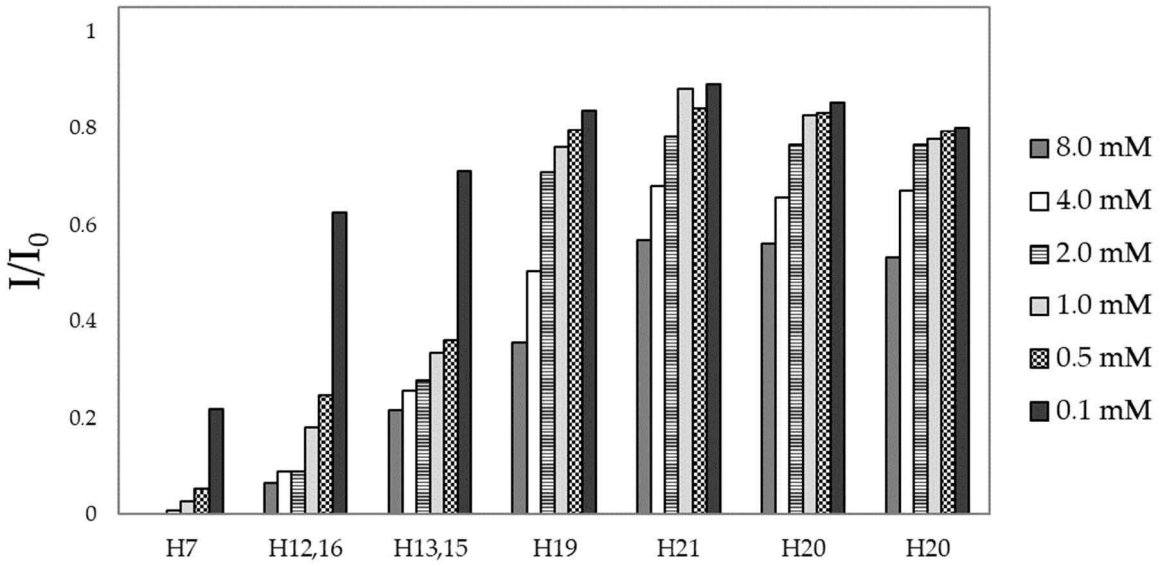

Figure 3. I/I_0 of FA protons at different concentrations. I and I_0 correspond to the intensity of the NMR signal in the presence and in absence of 0.02 Cu^{2+} eqs, respectively.

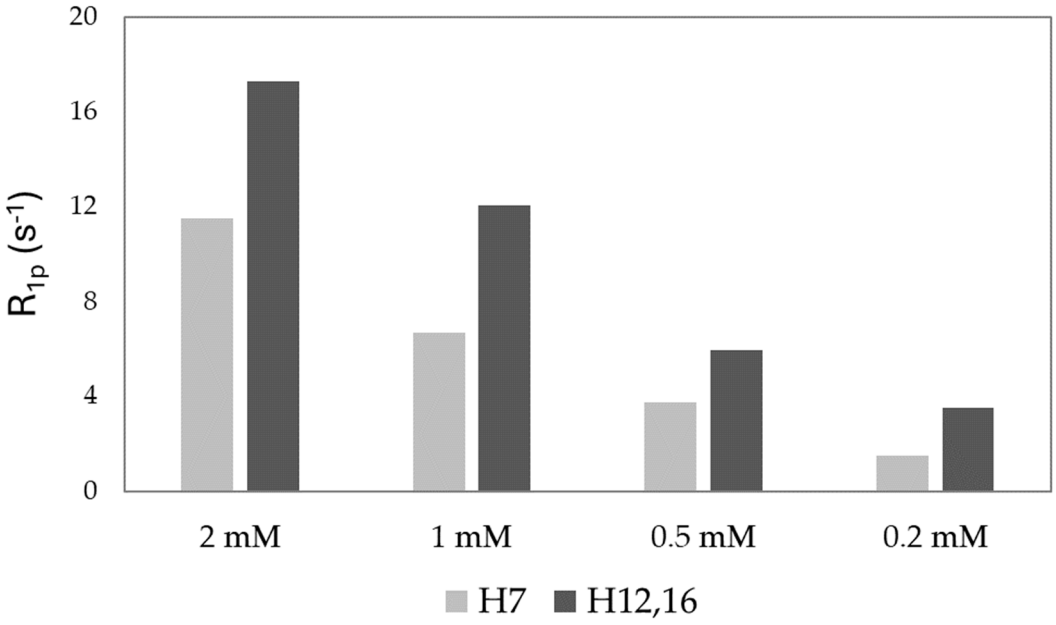

Figure 4. R_{1p} (s^{-1}) values of H7 and H12,16 protons of FA calculated in presence of 0.02 Cu^{2+} eqs.

The FA-Cu^{2+} binding was also studied at lower pH values to evaluate the role played by Glu carboxylates under acidic conditions. As shown in Figure 5, copper addition caused the complete disappearance of the H7 signal and significant broadening of the H12,16 signals at lower pH values as well. On the other hand, the acidification of the solution resulted in a shift of the Glu signals, which, as expected, are affected by the corresponding Glu pKa, without any change in line broadening. The low signal intensity observed at pH 5.0 is not dependent on the effect of copper but is rather due to the precipitation of FA occurring at low pH [52].

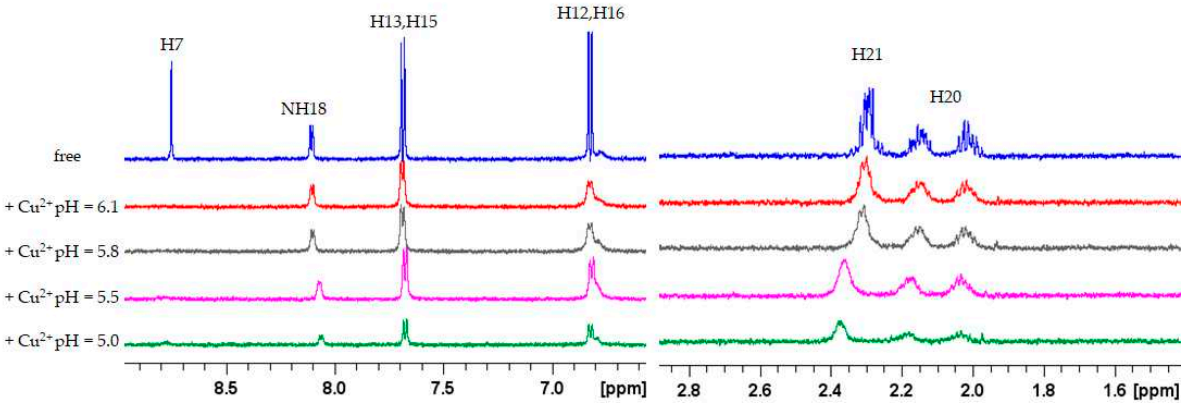

Figure 5. ^{1}H NMR spectra of FA 0.5 mM in H_2O/D_2O (9:1), T 298 K in absence (blue) and in presence of 0.02 Cu^{2+} eqs.; pH 6.1 (red), pH 5.8 (gray), pH 5.5 (magenta), pH 5.0 (green).

To gain deeper insights into the structural characteristics of the copper coordination sphere, ^{1}H-^{13}C HMBC spectra were recorded. This technique helped to identify the carbon atoms most influenced by the paramagnetic ions. Since the PTE ring has only one aromatic proton, relying solely on ^{1}H NMR spectra provides limited information, making the use of ^{1}H-^{13}C HMBC spectra crucial for better characterization.

As evident in Figure 6, copper(II) binding causes extensive line broadening on cross-peaks corresponding to C6, C7, C8a, C11, C12, C16, and C21. The comparison between the spectra obtained in the absence and presence of Cu^{2+} confirms that the most significant effects are localized on the PTE ring rather than on the Glu moiety. In particular, the ^{1}H and ^{13}C nuclei more influenced by the paramagnetic ions indicate N5 and carbonyl oxygen at position 4 as the copper donor atoms, in agreement with the results previously obtained for metal complexes containing pteridine ring [40,41,43,44].

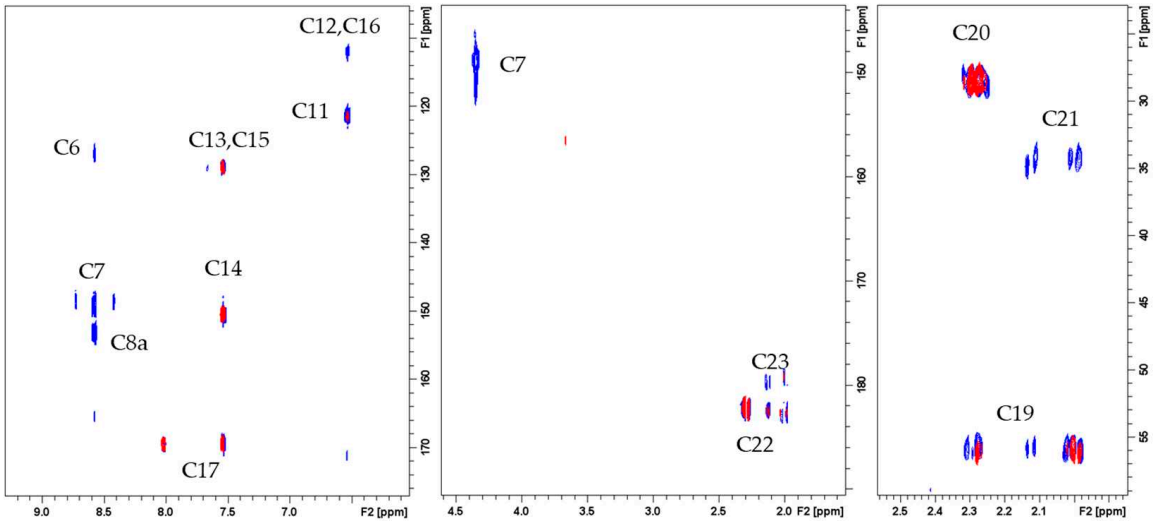

Figure 6. ^{1}H-^{13}C HMBC spectra of FA 10 mM, phosphate buffer 0.1 M, pH 7.35, T = 298 K in absence (blue contours) and in the presence of 0.01 Cu^{2+} eqs (red contours).

Based on the copper-induced effects observed in the NMR resonances, the models for both the mono and bis metal complexes are illustrated in Scheme 2.

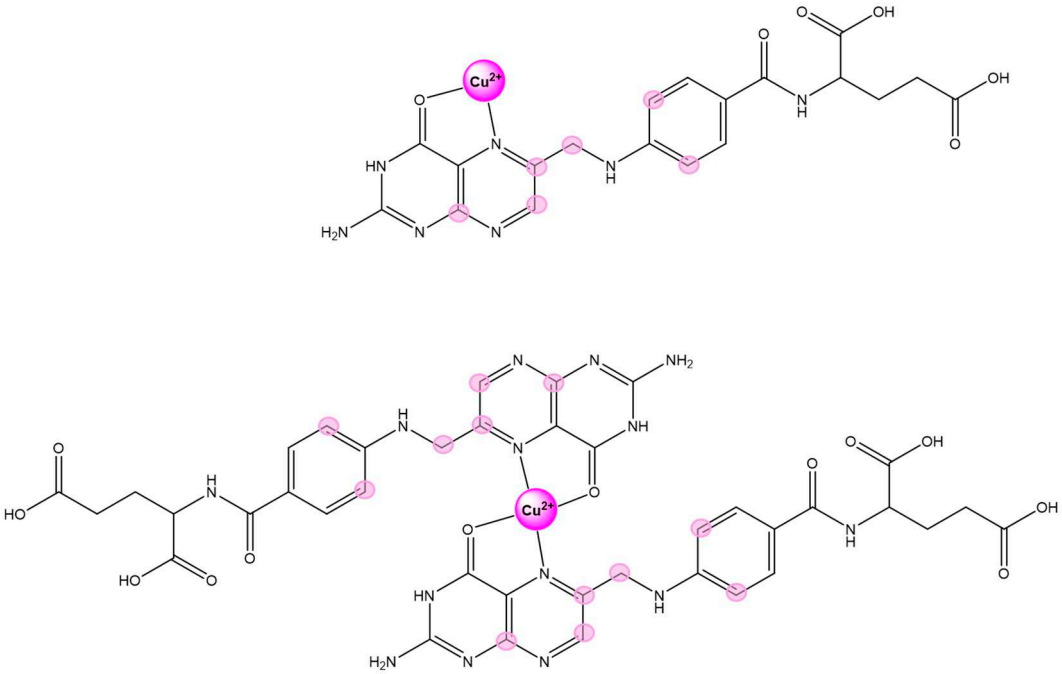

Scheme 2. Proposed structural models of mono and bis FA-Cu^{2+} complexes. The nuclei exhibiting the largest paramagnetic effects are highlighted in magenta.

3. Discussion

While folate synthesis is possible in most bacteria, yeast, and plants, animals need to obtain folate through their diet. In adults, a lack of dietary folate can result in anemia. For developing fetuses, inadequate folate intake increases the risk of birth defects known as neural tube defects, which occur due to incomplete closure of the neural tube early in pregnancy. Folic acid (vitamin B9) is also a common synthetic food additive used as a supplement of dietary folate [53].

In adults, folic acid is intimately involved in the synthesis of several key neurotransmitters: serotonin, dopamine, and noradrenaline, which are associated with depression, reward, attention, response to stress, and mood regulation [54]. A deficiency in folic acid can reduce the levels of these neurotransmitters, leading to issues with focus, adaptation, and mood stability. In adults, a deficiency in folate has been consistently linked to symptoms of depression and cognitive decline [55]. Moreover, FA influences the metabolism of homocysteine, an amino acid that, at high levels, is linked to an increased risk of AD [56]. Elevated homocysteine levels can enhance the production of amyloidogenic proteins, thus contributing to plaque formation [57,58].

Copper is an essential trace element that plays a critical role in brain function [59]. It is involved in the synthesis of neurotransmitters, antioxidant defense, and the maintenance of brain health. However, imbalances in copper levels can have significant implications. Copper is a cofactor for dopamine β-hydroxylase, the enzyme that converts dopamine to norepinephrine. Adequate copper levels are necessary for the production of norepinephrine, similar to the role of FA. Copper is a component of the antioxidant enzyme superoxide dismutase (SOD), which helps protect cells from oxidative stress [60]. Copper excess is more common and toxic to the brain and different studies show higher copper levels in individuals with depression. Additionally, increased copper levels in pregnant women, due to elevated progesterone and estrogen, may contribute to depression [59].

In this study, the structural characterization of FA-Cu^{2+} interaction in aqueous solution at physiological pH have been investigated by using NMR spectroscopy. Both folic acid and copper are essential micronutrients; the former is vital for DNA synthesis, cell division, and DNA methylation, while copper is a key component of numerous enzymes involved in redox reactions, energy production, connective tissue formation, and neurotransmission.

Our NMR findings strongly suggest that Cu^{2+} ions bind to folic acid through the N/O donor atoms of the PTE ring, excluding the involvement of Glu carboxylates in metal coordination. This conclusion is supported by the absence of effects on both ^{1}H and ^{13}C nuclei of Glu in all our NMR experiments. In contrast, previous solid-state studies on FA-Cu^{2+} complexes indicated that carboxylates coordinate to the cupric ion, forming bis or mononuclear complexes [35,37]. These discrepancies may be due to the high concentrations of FA ($\geq$100 mM) used in those studies, which likely caused the copper to anchor to different donor atoms, resulting in the formation of distinct copper complexes.

Our data, as shown by chemical shift variations and D values at increasing FA concentrations (Tables 1 and S1), reveal that intermolecular interactions between FA molecules occur at concentrations greater than 2 mM, hindering the access of metal ions to the PTE-binding sites. This is further confirmed by the paramagnetic effects observed at different FA concentrations (Figures 3 and 4). Specifically, the data indicate that, while maintaining an identical FA–metal ratio, higher FA concentrations result in more significant metal-induced effects. Moreover, despite variations in intensity, the trend remains consistent, with H7, H12, and H16 being the most affected protons in all cases. This suggests that similar copper coordination occurs independently of the concentrations investigated, differing only in kinetic parameters. As previously reported for Cu^{2+} binding to histidine containing peptides, the kinetic off-rate (k_{off}) significantly impacts copper-induced line broadening and it can be correlated with the strength of the metal–ligand associations, with a slower exchange rate being obviously correlated with a stronger copper binding [61].

For these reasons, it is reasonable to assume that copper binding to FA is strongly concentration dependent. Therefore, at low FA concentrations, which are typically found in the human body and physiological environments, copper is likely to anchor to the PTE ring. This ring is well known for forming stable mono and bis Cu^{2+} complexes in various PTE-containing systems [41]. In all the previously investigated systems, copper(II) is able to form a stable planar five membered chelated ring by coordinating the O4 and N5 donor atoms. This binding mode is also preserved in copper complexes with dimethyllumazine, a methylated pteridine-2,4(1H,3H)-dione compound capable of forming both copper mononuclear and bis complexes [43,62]. Copper binding to the N4 and O5 atoms results in a well-defined Cu-H7 distance of 4.97 Å, as determined by the X-ray structure published by Hueso-Hurena et al. [62]. Given the homology of the copper coordination sphere and the structural similarity of the PTE ring, a Cu-H7 distance of about 5 Å can be surmised in the FA-Cu^{2+} complexes investigated in this study. Assuming this is the case, the kinetic off-rate values of the FA-Cu^{2+} complexes can be evaluated from the paramagnetic relaxation enhancement (R_{1p}) by employing an approach similar to those previously published for Cu^{2+} complexes with His-containing peptides [61]. In particular, it is well known that in solutions containing ligands with paramagnetic ions as co-solutes, the measured spin-lattice relaxation rate is averaged over the values from free (f) and metal-bound (b) environments, where p_f and p_b represent the fractional population and k_{off} is the kinetic rate constant for exit from the metal coordination sphere [63,64].

$$R_{1p} = R_{1obs} - p_f R_{1f} = p_b / \left(T_{1b} + k_{off}^{-1}\right) \quad (1)$$

R_{1b} ($1/T_{1b}$) is the structure sensitive term, described by the Solomon equation [65], which can be calculated from the R_{1p} values when determining the metal nucleus distances. At the same time, Equation (1) indicates that the exchange rate may become a limiting factor, potentially diminishing the paramagnetic contribution to spin-lattice relaxation rates and, similarly, affecting the line width. As previously described [61] R_{1b} can be calculated for a proton at a fixed distance from the metal and then inserted into Equation (1) to determine the k_{off} values. In particular, the assumed Cu-H7 distance of 5 Å ($R_{1b} \approx 550\ s^{-1}$) has provided the exchange rates reported in Table 2. These rates were then employed to calculate the Cu-H12,16 distances for all the investigated complexes. The results indicate varying kinetic rates depending on concentration, with slower rates observed at the lowest

concentration (0.2 mM). Additionally, the kinetic rates were used to determine the distances between copper and H12,16 nuclei. As shown by the calculated values, lower concentrations correspond to shorter distances, suggesting that the PABA ring is moving closer to the copper center, potentially stabilizing and protecting the copper coordination sphere. This behavior aligns with the slower kinetic rates and suggests that at low concentrations, PABA, less engaged in intermolecular associations, remains more available for interactions with copper ions.

Table 2. R_{1p}, k_{off} and Cu-H distances of FA calculated at different concentrations, phosphate buffer 20 mM, T 298 K.

C_M (mmolL^{-1})	R_{1p} (s^{-1})		k_{off} (s^{-1})	$d_{Cu\text{-}H12,16}$ (Å)
	H7	H12,16		
0.2 mM	1.50	3.48	178	3.28
0.5 mM	3.73	5.93	310	3.37
1.0 mM	6.67	12.05	1000	4.21
2.0 mM	11.52	17.26	10,000	4.56

4. Materials and Methods

Folic acid (Sigma-Aldrich, Schnelldorf, Germany) was dissolved in deionized water containing D_2O 10% or in deuterium oxide. The samples recorded at physiological pH were prepared by using phosphate buffer 20 mM or 1 M (Sigma-Aldrich, Schnelldorf, Germany). For the samples without a buffer, the pH was adjusted at desired values with either DCl or NaOD. The desired concentration of copper ions was achieved by using a stock aqueous solution of copper sulfate 0.2 M (Sigma-Aldrich, Schnelldorf, Germany). TMSP-d4 (Sigma-Aldrich, Schnelldorf, Germany), 3-(trimethylsilyl)-[2,2,3,3-d4] propansulfonate sodium salt, was used as an internal reference standard.

All the NMR experiments were carried out at 14.1 T with a Bruker Avance III 600 MHz spectrometer at controlled temperature (298 K). A 5 mm broadband inverse (BBI) probe was used for all the experiments. Suppression of the residual water signal was achieved by excitation sculpting using a selective square pulse on water 2 ms long [66].

A standard NMR spectrum was acquired using 16 transients, with a spectral width of 7200 Hz and a recycle delay of 2.0 s. Proton resonance assignments for folic acid were determined through TOCSY and NOESY experiments. For TOCSY, a total spin-locking duration of 60 ms was employed using the MLEV-17 mixing sequence. NOESY spectra were collected with varying mixing times to identify the optimal conditions. Data processing was carried out with TopSpin 3.6 software. The proton spin-lattice relaxation rates were obtained using an inversion recovery pulse sequence, with all rates derived from regression analysis of the longitudinal magnetization recovery curves, ensuring errors did not exceed 3%.

The diffusion coefficients were measured at 298 K using a PFG longitudinal eddy-current delay (LED) pulse sequence, incorporating bipolar gradients with spoil gradients during the longitudinal storage period [67]. The gradient strength was varied, starting from 0.86 Gcm^{-1} with a step size of 2.65 Gcm^{-1} over 2 ms, while maintaining constant field gradient separations and total echo time. A set of 16 2D spectra was recorded for each measurement, with scan numbers ranging from 16 to 256 and a recycle time of 10 s between scans. Diffusion values were determined by analyzing signal decay via regression, resulting in errors no greater than ±2–5%.

5. Conclusions

Folic acid and copper are indispensable micronutrients with essential roles in various physiological processes, including DNA synthesis, cell division, and neurotransmitter function. This study provides new insights into the interaction between folic acid and copper(II) ions, highlighting the concentration-dependent nature of their binding. Using

NMR spectroscopy, we elucidated that copper binds primarily to the pteridine ring of folic acid, with minimal involvement of the glutamic acid moiety. This finding contrasts with earlier studies that suggested significant coordination through carboxylate groups at high folic acid concentrations. Our results show that at physiological levels of folic acid, copper predominantly interacts with the pteridine ring, supported by interactions with the p-aminobenzoic acid ring at lower concentrations.

This study also revealed that the binding of copper to folic acid is highly sensitive to concentration variations. At low folic acid concentrations, the pteridine ring is the major binding site, and interactions with the PABA ring enhance the stability of the copper complex. This concentration-dependent binding suggests that copper and folic acid may have synergistic or antagonistic effects depending on their relative concentrations in biological systems.

These findings have significant implications for understanding the bioavailability and effectiveness of these micronutrients in the body. They suggest that copper's interaction with folic acid could influence its role in various metabolic pathways and may affect the efficiency of folic acid supplementation, especially in populations at risk of deficiencies or with specific health conditions. Future research should further explore the dynamic interactions between folic acid and copper, assessing how these interactions impact overall nutrient function and disease prevention. This deeper understanding could lead to improved dietary recommendations and targeted supplementation strategies to enhance health outcomes.

Supplementary Materials: The following supporting information can be downloaded at: https://www.mdpi.com/article/10.3390/inorganics12090248/s1, Table S1: NMR Chemical Shift assignments of FA at different concentrations in 20 mM phosphate buffer at pH 7.35; Figure S1: pH dependence of proton chemical shift of FA 0.5 mM: A. Superimposition of ^{1}H NMR signals of H7 and H12,16 at different pH values starting from 6.15 to 8.05; B. Chemical shift variations of FA protons at different pH values; Figure S2: ^{1}H NMR spectra of FA 0.5 mM in phosphate buffer 20 mM (pH 7.35) and T = 298 K in absence and in presence of Fe^{3+} ions. Fe^{3+} = 0 eqs (blue); Fe^{3+} = 0.02 eqs (red); Fe^{3+} = 0.04 eqs (gray); Fe^{3+} = 0.08 eqs (magenta); Fe^{3+} = 0.12 eqs (green); Fe^{3+} = 0.20 eqs (light blue); Figure S3: ^{1}H NMR spectra of FA 0.5 mM in phosphate buffer 20 mM (pH 7.35) and T = 298 K in absence and in presence of Fe^{2+} ions. Fe^{2+} = 0 eqs (blue); Fe^{2+} = 0.02 eqs (red); Fe^{2+} = 0.04 eqs (gray); Fe^{2+} = 0.08 eqs (magenta); Fe^{2+} = 0.12 eqs (green); Fe^{2+} = 0.20 eqs (light blue); Figure S4: ^{1}H NMR spectra of FA 0.5 mM in phosphate buffer 20 mM (pH 7.35) and T = 298 K in absence and in presence of Zn^{2+} ions. Zn^{2+} = 0 eqs (blue); Zn^{2+} = 0.3 eqs (red); Zn^{2+} = 0.6 eqs (gray); Zn^{2+} = 0.9 eqs (magenta).

Author Contributions: Conceptualization, A.K. and D.V.; methodology, A.K. and D.V.; software, A.K.; validation, A.K. and D.V.; formal analysis, D.V.; investigation, A.K.; resources, A.K. and D.V.; data curation, A.K. and D.V.; writing—original draft preparation, A.K. and D.V.; writing—review and editing, A.K. and D.V.; visualization, A.K. and D.V.; supervision, A.K. and D.V.; project administration, A.K. and D.V.; funding acquisition, A.K. and D.V. All authors have read and agreed to the published version of the manuscript.

Funding: This research was funded by MUR-PRIN 2022 grant number 2022RCRWE5.

Data Availability Statement: Data are contained within the article and Supplementary Materials.

Acknowledgments: The Consorzio Interuniversitario Risonanze Magnetiche di Metallo Proteine (CIRMMP) is acknowledged for the scholarship support.

Conflicts of Interest: The authors declare no conflicts of interest.

References

1. Hoffbrand, A.V.; Weir, D.G. The History of Folic Acid. *Br. J. Haematol.* **2001**, *113*, 579–589. [CrossRef] [PubMed]
2. Zheng, Y.; Cantley, L.C. Toward a Better Understanding of Folate Metabolism in Health and Disease. *J. Exp. Med.* **2019**, *216*, 253–266. [CrossRef] [PubMed]

3. Blakley: Nomenclature and Symbols for Folic Acid...—Google Scholar. Available online: https://scholar.google.com/scholar_lookup?title=Nomenclature%20and%20symbols%20for%20folic%20acid%20and%20related%20compounds.%20Recommendations&publication_year=1986&author=R.L.%20Blakley&author=IUPAC-IUB%20Joint%20Commission%20on%20Biochemical%20Nomenclature%20(JCBN) (accessed on 6 June 2024).
4. Saini, R.K.; Nile, S.H.; Keum, Y.-S. Folates: Chemistry, Analysis, Occurrence, Biofortification and Bioavailability. *Food Res. Int.* **2016**, *89*, 1–13. [CrossRef] [PubMed]
5. Mahara, F.A.; Nuraida, L.; Lioe, H.N.; Nurjanah, S. Hypothetical Regulation of Folate Biosynthesis and Strategies for Folate Overproduction in Lactic Acid Bacteria. *Prev. Nutr. Food Sci.* **2023**, *28*, 386–400. [CrossRef] [PubMed]
6. Fox, J.T.; Stover, P.J. Chapter 1 Folate-Mediated One-Carbon Metabolism. In *Vitamins & Hormones*; Folic Acid and Folates; Academic Press: Cambridge, MA, USA, 2008; Volume 79, pp. 1–44.
7. Menezo, Y.; Elder, K.; Clement, A.; Clement, P. Folic Acid, Folinic Acid, 5 Methyl TetraHydroFolate Supplementation for Mutations That Affect Epigenesis through the Folate and One-Carbon Cycles. *Biomolecules* **2022**, *12*, 197. [CrossRef]
8. Wang, Q.; Zhao, J.; Chang, H.; Liu, X.; Zhu, R. Homocysteine and Folic Acid: Risk Factors for Alzheimer's Disease—An Updated Meta-Analysis. *Front. Aging Neurosci.* **2021**, *13*, 665114. [CrossRef]
9. Seshadri, S. Homocysteine and the Risk of Dementia. *Clin. Chem.* **2012**, *58*, 1059–1060. [CrossRef]
10. Zhang, X.; Bao, G.; Liu, D.; Yang, Y.; Li, X.; Cai, G.; Liu, Y.; Wu, Y. The Association Between Folate and Alzheimer's Disease: A Systematic Review and Meta-Analysis. *Front. Neurosci.* **2021**, *15*, 661198. [CrossRef]
11. Price, B.R.; Wilcock, D.M.; Weekman, E.M. Hyperhomocysteinemia as a Risk Factor for Vascular Contributions to Cognitive Impairment and Dementia. *Front. Aging Neurosci.* **2018**, *10*, 350. [CrossRef]
12. Spence, J.D. Nutrition and Risk of Stroke. *Nutrients* **2019**, *11*, 647. [CrossRef]
13. Dang, S.; Jain, A.; Dhanda, G.; Bhattacharya, N.; Bhattacharya, A.; Senapati, S. One Carbon Metabolism and Its Implication in Health and Immune Functions. *Cell Biochem. Funct.* **2024**, *42*, e3926. [CrossRef] [PubMed]
14. US Preventive Services Task Force. Folic Acid Supplementation to Prevent Neural Tube Defects: US Preventive Services Task Force Reaffirmation Recommendation Statement. *JAMA* **2023**, *330*, 454–459. [CrossRef] [PubMed]
15. Pietrzik, K.; Bailey, L.; Shane, B. Folic Acid and L-5-Methyltetrahydrofolate. *Clin. Pharmacokinet.* **2010**, *49*, 535–548. [CrossRef] [PubMed]
16. Nazki, F.H.; Sameer, A.S.; Ganaie, B.A. Folate: Metabolism, Genes, Polymorphisms and the Associated Diseases. *Gene* **2014**, *533*, 11–20. [CrossRef] [PubMed]
17. Zhang, N.; Zhou, Z.; Chi, X.; Fan, F.; Li, S.; Song, Y.; Zhang, Y.; Qin, X.; Sun, N.; Wang, X.; et al. Folic Acid Supplementation for Stroke Prevention: A Systematic Review and Meta-Analysis of 21 Randomized Clinical Trials Worldwide. *Clin. Nutr.* **2024**, *43*, 1706–1716. [CrossRef]
18. Espinosa-Salas, S.; Gonzalez-Arias, M. Nutrition: Micronutrient Intake, Imbalances, and Interventions. In *StatPearls*; StatPearls Publishing: Treasure Island, FL, USA, 2024.
19. Centeno Tablante, E.; Pachón, H.; Guetterman, H.M.; Finkelstein, J.L. Fortification of Wheat and Maize Flour with Folic Acid for Population Health Outcomes. *Cochrane Database Syst. Rev.* **2019**, *7*, CD012150. [CrossRef]
20. Zeng, R.; Xu, C.-H.; Xu, Y.-N.; Wang, Y.-L.; Wang, M. The Effect of Folate Fortification on Folic Acid-Based Homocysteine-Lowering Intervention and Stroke Risk: A Meta-Analysis. *Public. Health Nutr.* **2015**, *18*, 1514–1521. [CrossRef]
21. Moustakas, M. The Role of Metal Ions in Biology, Biochemistry and Medicine. *Materials* **2021**, *14*, 549. [CrossRef]
22. Singh, R.; Panghal, A.; Jadhav, K.; Thakur, A.; Verma, R.K.; Singh, C.; Goyal, M.; Kumar, J.; Namdeo, A.G. Recent Advances in Targeting Transition Metals (Copper, Iron, and Zinc) in Alzheimer's Disease. *Mol. Neurobiol.* **2024**, 1–25. [CrossRef]
23. Wang, X.; Wang, X.; Guo, Z. Metal-Involved Theranostics: An Emerging Strategy for Fighting Alzheimer's Disease. *Coord. Chem. Rev.* **2018**, *362*, 72–84. [CrossRef]
24. Kola, A.; Nencioni, F.; Valensin, D. Bioinorganic Chemistry of Micronutrients Related to Alzheimer's and Parkinson's Diseases. *Molecules* **2023**, *28*, 5467. [CrossRef] [PubMed]
25. Wang, B.; Fang, T.; Chen, H. Zinc and Central Nervous System Disorders. *Nutrients* **2023**, *15*, 2140. [CrossRef] [PubMed]
26. An, Y.; Li, S.; Huang, X.; Chen, X.; Shan, H.; Zhang, M. The Role of Copper Homeostasis in Brain Disease. *Int. J. Mol. Sci.* **2022**, *23*, 13850. [CrossRef] [PubMed]
27. Gaggelli, E.; Kozlowski, H.; Valensin, D.; Valensin, G. Copper Homeostasis and Neurodegenerative Disorders (Alzheimer's, Prion, and Parkinson's Diseases and Amyotrophic Lateral Sclerosis). *Chem. Rev.* **2006**, *106*, 1995–2044. [CrossRef] [PubMed]
28. Tyczyńska, M.; Gędek, M.; Brachet, A.; Stręk, W.; Flieger, J.; Teresiński, G.; Baj, J. Trace Elements in Alzheimer's Disease and Dementia: The Current State of Knowledge. *J. Clin. Med.* **2024**, *13*, 2381. [CrossRef]
29. Kozlowski, H.; Luczkowski, M.; Remelli, M.; Valensin, D. Copper, Zinc and Iron in Neurodegenerative Diseases (Alzheimer's, Parkinson's and Prion Diseases). *Coord. Chem. Rev.* **2012**, *256*, 2129–2141. [CrossRef]
30. Lachowicz, J.I.; Lecca, L.I.; Meloni, F.; Campagna, M. Metals and Metal-Nanoparticles in Human Pathologies: From Exposure to Therapy. *Molecules* **2021**, *26*, 6639. [CrossRef]
31. Kardos, J.; Héja, L.; Simon, Á.; Jablonkai, I.; Kovács, R.; Jemnitz, K. Copper Signalling: Causes and Consequences. *Cell Commun. Signal.* **2018**, *16*, 71. [CrossRef]
32. Catalani, S.; Paganelli, M.; Gilberti, M.E.; Rozzini, L.; Lanfranchi, F.; Padovani, A.; Apostoli, P. Free Copper in Serum: An Analytical Challenge and Its Possible Applications. *J. Trace Elem. Med. Biol.* **2018**, *45*, 176–180. [CrossRef]

33. Li, X.; Chen, X.; Gao, X. Copper and Cuproptosis: New Therapeutic Approaches for Alzheimer's Disease. *Front. Aging Neurosci.* **2023**, *15*, 1300405. [CrossRef]
34. Bagheri, S.; Squitti, R.; Haertlé, T.; Siotto, M.; Saboury, A.A. Role of Copper in the Onset of Alzheimer's Disease Compared to Other Metals. *Front. Aging Neurosci.* **2018**, *9*. [CrossRef] [PubMed]
35. Hamed, E.; Attia, M.S.; Bassiouny, K. Synthesis, Spectroscopic and Thermal Characterization of Copper(II) and Iron(III) Complexes of Folic Acid and Their Absorption Efficiency in the Blood. *Bioinorg. Chem. Appl.* **2009**, *2009*, 979680. [CrossRef] [PubMed]
36. Skorik, N.A. D-Metal Folates and the Folic Acid-Imidazole Conjugate. *Russ. J. Inorg. Chem.* **2015**, *60*, 1402–1406. [CrossRef]
37. Dametto, P.R.; Ambrozini, B.; Caires, F.J.; Franzini, V.P.; Ionashiro, M. Synthesis, Characterization and Thermal Behaviour of Solid-State Compounds of Folates with Some Bivalent Transition Metals Ions. *J. Therm. Anal. Calorim.* **2014**, *115*, 161–166. [CrossRef]
38. El-Wahed, M.G.A.; Refat, M.S.; El-Megharbel, S.M. Synthesis, Spectroscopic and Thermal Characterization of Some Transition Metal Complexes of Folic Acid. *Spectrochim. Acta-Part. A Mol. Biomol. Spectrosc.* **2008**, *70*, 916–922. [CrossRef]
39. Refat, M.S.; Altalhi, T.; Hassan, R.F. Synthesis, Spectroscopic, Structural and Morphological Characterizations of Magnesium(II), Calcium(II), Strontium(II) and Barium(II) Folate Complexes. *J. Mol. Struct.* **2021**, *1227*, 129519. [CrossRef]
40. Hueso-Ureña, F.; Jiménez-Pulido, S.B.; Moreno-Carretero, M.N.; Qòs-Olozàbal, M.; Salas-Peregrìn, J.M. A New Three-Dimensional, Hydrogen-Bonded Metal-Pteridine Complex: Synthesis, Characterization and Crystal Structure of Diaqua Bis(1,3-Dimethylpteridine-2,4(1*H*,3*H*)-Dione-*O*4,*N*5) Copper(II) Nitrate Dihydrate. *Polyhedron* **1997**, *16*, 607–612. [CrossRef]
41. Kaim, W.; Schwederski, B.; Heilmann, O.; Hornung, F.M. Coordination Compounds of Pteridine, Alloxazine and Flavin Ligands: Structures and Properties. *Coord. Chem. Rev.* **1999**, *182*, 323–342. [CrossRef]
42. Kohzuma, T.; Morita, Y.; Takani, M.; Odani, A.; Yamauchi, O. Pteridine-Containing Ternary Copper (II) Complexes as Pterin Cofactor-Metal Binding Models. Structures, Solution Equilibria, and Redox Activities. *Inorg. Chem.* **1988**, *27*, 3854–3858. [CrossRef]
43. Acuña-Cueva, E.R.; Faure, R.; Illán-Cabeza, N.A.; Jiménez-Pulido, S.B.; Moreno-Carretero, M.N.; Quirós-Olozábal, M. Synthesis and Characterization of Several Lumazine Derivative Complexes of Co(II), Ni(II), Cu(II), Cd(II), Pd(II) and Pt(II). X-ray Structures of a Mononuclear Copper Complex and a Dinuclear Cadmium Complex. *Inorganica Chim. Acta* **2003**, *351*, 356–362. [CrossRef]
44. Acuña-Cueva, E.R.; Faure, R.; Illán-Cabeza, N.A.; Jiménez-Pulido, S.B.; Moreno-Carretero, M.N.; Quirós-Olozábal, M. Synthesis and Structural Studies on New MIIX2L2 Dihalocomplexes of 1-Methyllumazine and 1,6,7-Trimethyllumazine. *Polyhedron* **2003**, *22*, 483–488. [CrossRef]
45. Lam, Y.-F.; Kotowycz, G. Self Association of Folic Acid in Aqueous Solution by Proton Magnetic Resonance. *Can. J. Chem.* **1972**, *50*, 2357–2363. [CrossRef]
46. Rosbottom, I.; Turner, T.D.; Ma, C.Y.; Hammond, R.B.; Roberts, K.J.; Yong, C.W.; Todorov, I.T. The Structural Pathway from Its Solvated Molecular State to the Solution Crystallisation of the α- and β-Polymorphic Forms of Para Amino Benzoic Acid. *Faraday Discuss.* **2022**, *235*, 467–489. [CrossRef] [PubMed]
47. Kola, A.; Vigni, G.; Baratto, M.C.; Valensin, D. A Combined NMR and UV-Vis Approach to Evaluate Radical Scavenging Activity of Rosmarinic Acid and Other Polyphenols. *Molecules* **2023**, *28*, 6629. [CrossRef] [PubMed]
48. Kola, A.; Vigni, G.; Valensin, D. Exploration of Lycorine and Copper(II)'s Association with the N-Terminal Domain of Amyloid β. *Inorganics* **2023**, *11*, 443. [CrossRef]
49. De Ricco, R.; Potocki, S.; Kozlowski, H.; Valensin, D. NMR Investigations of Metal Interactions with Unstructured Soluble Protein Domains. *Coord. Chem. Rev.* **2014**, *269*, 1–12. [CrossRef]
50. Kola, A.; Hecel, A.; Lamponi, S.; Valensin, D. Novel Perspective on Alzheimer's Disease Treatment: Rosmarinic Acid Molecular Interplay with Copper(II) and Amyloid β. *Life* **2020**, *10*, 118. [CrossRef]
51. Dudek, D.; Miller, A.; Hecel, A.; Kola, A.; Valensin, D.; Mikolajczyk, A.; Barcelo-Oliver, M.; Matera-Witkiewicz, A.; Rowinnska-Zyrek, M. Semenogelins Armed in Zn(II) and Cu(II): May Bioinorganic Chemistry Help Nature to Cope with *Enterococcus Faecalis*? *Inorg. Chem.* **2023**, *62*, 14103–14115. [CrossRef]
52. Wu, Z.; Li, X.; Hou, C.; Qian, Y. Solubility of Folic Acid in Water at pH Values between 0 and 7 at Temperatures (298.15, 303.15, and 313.15) K. *J. Chem. Eng. Data* **2010**, *55*, 3958–3961. [CrossRef]
53. Ducker, G.S.; Rabinowitz, J.D. One-Carbon Metabolism in Health and Disease. *Cell Metab.* **2017**, *25*, 27–42. [CrossRef]
54. Fava, M.; Mischoulon, D. Folate in Depression: Efficacy, Safety, Differences in Formulations, and Clinical Issues. *J. Clin. Psychiatry* **2009**, *70*, 12–17. [CrossRef] [PubMed]
55. Reynolds, E. Vitamin B12, Folic Acid, and the Nervous System. *Lancet Neurol.* **2006**, *5*, 949–960. [CrossRef] [PubMed]
56. Smith, A.D.; Refsum, H. Homocysteine, B Vitamins, and Cognitive Impairment. *Annu. Rev. Nutr.* **2016**, *36*, 211–239. [CrossRef] [PubMed]
57. Shen, L.; Ji, H.-F. Associations between Homocysteine, Folic Acid, Vitamin B12 and Alzheimer's Disease: Insights from Meta-Analyses. *J. Alzheimer's Dis.* **2015**, *46*, 777–790. [CrossRef]
58. Lee, C.-Y.; Chan, L.; Hu, C.-J.; Hong, C.-T.; Chen, J.-H. Role of Vitamin B12 and Folic Acid in Treatment of Alzheimer's Disease: A Meta-Analysis of Randomized Control Trials. *Aging* **2024**, *16*, 7856–7869. [CrossRef]
59. Chen, J.; Song, W.; Zhang, W. The Emerging Role of Copper in Depression. *Front. Neurosci.* **2023**, *17*, 1230404. [CrossRef]
60. Gale, J.; Aizenman, E. The Physiological and Pathophysiological Roles of Copper in the Nervous System. *Eur. J. Neurosci.* **2024**, *60*, 3505–3543. [CrossRef]

61. Gaggelli, E.; Kozlowski, H.; Valensin, D.; Valensin, G. NMR Studies on Cu(II)-Peptide Complexes: Exchange Kinetics and Determination of Structures in Solution. *Mol. Biosyst.* **2005**, *1*, 79–84. [CrossRef]
62. Hueso-Ureña, F.; Jiménez-Pulido, S.B.; Moreno-Carretero, M.N.; Quirós-Olozábal, M.; Salas-Peregrín, J.M. Synthesis and Structural Studies on New M IIX2L2 Dihalocomplexes of 1,3-Dimethyllumazine and 1,3,6,7-Tetramethyllumazine. Crystal Structure of the Monodimensionally Hydrogen-Bonded Dichloro-Bis (1,3-Dimethylpteridine-2,4 (1H,3H)-Dione-O 4,N 5) Copper (II) Dihydrate. *Polyhedron* **1998**, *18*, 85–91. [CrossRef]
63. Bertini, I.; Luchinat, C. *NMR of Paramagnetic Substances*; Elsevier: Amsterdam, The Netherlands, 1996.
64. Gaggelli, E.; D'Amelio, N.; Valensin, D.; Valensin, G. 1H NMR Studies of Copper Binding by Histidine-Containing Peptides. *Magn. Reson. Chem.* **2003**, *41*, 877–883. [CrossRef]
65. Solomon, I. Relaxation Processes in a System of Two Spins. *Phys. Rev.* **1955**, *99*, 203–256. [CrossRef]
66. Hwang, T.L.; Shaka, A.J. Multiple-Pulse Mixing Sequences That Selectively Enhance Chemical Exchange or Cross-Relaxation Peaks in High-Resolution NMR Spectra. *J. Magn. Reson.* **1998**, *135*, 280–287. [CrossRef] [PubMed]
67. Johnson, C.S., Jr. ChemInform Abstract: Diffusion Ordered Nuclear Magnetic Resonance Spectroscopy: Principles and Applications. *ChemInform* **1999**, *30*, chin.199933338. [CrossRef]